89--J-2013-TPS--On the Electrical Characteristic of Atmospheric Pressure AirHeO-2N-2Ar Plasma Needle

Article · April 2018

CITATIONS
0

READS
41

1 author:

Xinpei Lu
Huazhong University of Science and Technology
165 PUBLICATIONS **42** CITATIONS

SEE PROFILE

On the Electrical Characteristic of Atmospheric Pressure Air/He/O_2/N_2/Ar Plasma Needle

Zilan Xiong, Quanjun Huang, Zhan Wang, Xinpei Lu, and Yuan Pan

***Abstract*— The electrical characteristics of an air plasma needle are investigated. The discharge is driven by pulsed direct current voltages. A series of discharge pulses appear for one applied voltage pulse. The interval between nearby discharge current is tens of nanoseconds, which corresponds to a frequency of tens of MHz. This is much higher than that of the Trichel pulse (tens of kHz). The frequency of the discharge current pulses increases with the applied voltage but decreases with the gas gap distance. The series current pulses are found not only existing in electronegative gases (air, pure O_2), but also in Ar and N_2. On the other hand, when He is used, there always appears only one discharge current pulse; by adding small percentage of O_2 to He, multiple discharges appear again.**

***Index Terms*— Atmospheric pressure plasma, biomedical application, nonequilibrium plasma, plasma jet.**

I. Introduction

ROOM temperature atmospheric pressure plasmas (RT-APPs) attract lots of attention because of their enhanced plasma chemistry without the need for elevated gas temperature [1]–[15]. For plasmas originating from gas discharge, the plasma chemistry is driven by electrons. The electrons gain energy from the electric field and then transfer part of the energy to molecules through collisions. Some of the molecules are excited, dissociated, or ionized, which makes the plasma very reactive while the gas temperature remains at low or even at RT. These attractive characteristics make them attractive for applications such as plasma medicine.

Traditionally, RT-APPs are generated in discharge gaps between two electrodes, which are inefficient or even impossible for applications, such as teeth root canal treatment and assistant wound healing. To overcome the shortcoming of the traditional RT-APPs mentioned above, various RT-APP jets (RT-APPJs) are developed [16]–[19]. The RT-APPJs generate plasmas in open space rather than in confined discharge gaps, which make it very convenient for applications such as plasma medicine. Recently, we have reported an RT-APPJs using air as working gas [20]. The plasma is driven by pulsed direct current (dc) voltages. It is found that there are multiple discharge current pulses for a single voltage pulse. The pulsewidth of each current pulse is $\sim$10 ns and the time between adjacent current pulses is $\sim$100 ns. These characteristics are very different from the traditional Trichel pulses in negative and positive pin-to-plane corona discharge in air. To understand more about the characteristics of the plasma, the effects of the amplitude of the applied voltage, pulse frequency, pulsewidth, and working gas (He, He+O_2, Ar, N_2, O_2, and air) on the current–voltage (I–V) characteristics of the plasma are investigated in this paper.

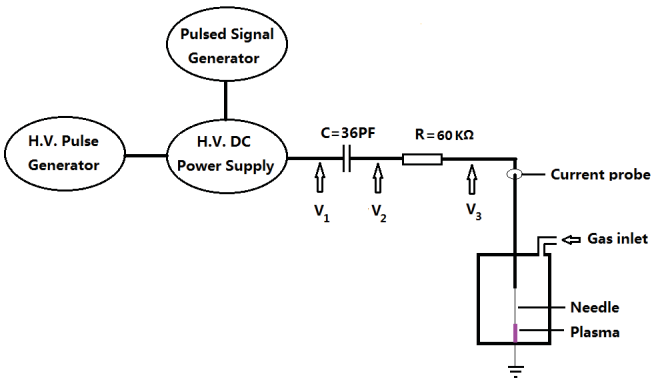

Fig. 1. Schematic view of the experimental setup.

II. Experimental Setup

Fig. 1 shows the schematic view of the device. The main body of the device comprises a stainless steel needle. The diameter of the stainless steel tip is $\sim$100 μm. The stainless steel needle serves as the electrode, which is connected to a high-voltage (HV) submicrosecond pulsed dc power supply through a 60-kΩ ballast resistor R and a 36-pF capacitor C. Both the resistor and the capacitor are used for controlling the discharge current and the voltage on the needle. Hence, the plasma can be touched by bare hands of human being without any feeling of heat or electrical shocking. The applied voltage V_1, the voltage after the capacitor V_2, and the voltage V_3 on the needle are measured by three P6015 Tektronix HV probes, respectively. The discharge currents are measured by a CT1 Tektronix current probe. The voltage and current waveforms are recorded by a Tektronix DPO7104 wideband digital oscilloscope. More detailed information about this device can be found in [20].

Manuscript received April 2, 2013; revised April 26, 2013; accepted April 26, 2013. Date of publication June 18, 2013; date of current version July 3, 2013. This work was supported in part by the National Natural Science Foundation under Grant 51077063 and Grant 51277087, the Research Fund for the Doctoral Program of Higher Education of China under Grant 20100142110005, and the Chang Jiang Scholars Program, Ministry of Education, People's Republic of China.

The authors are with the State Key Laboratory of Advanced Electromagnetic Engineering and Technology, Huazhong University of Science and Technology, Wuhan 430030, China (e-mail: 396915763@qq.com; hqj20090130@163.com; dlzys601@163.com; luxinpei@hotmail.com; panyuan@hust.edu.cn).

Color versions of one or more of the figures in this paper are available online at http://ieeexplore.ieee.org.

Digital Object Identifier 10.1109/TPS.2013.2265918

In this paper, to investigate the effect of working gas on the plasma characteristics, the needle is fixed inside a sealed quartz glass tube (innerdiameter of 2.5 cm) with the length of 10 cm. One end of the tube is sealed by a rubber stopper with a hole allow the working gases flowing. The bottom of the tube is covered with aluminum foil that acts as the ground electrode. The flow rate of all the gasses used is 200 sccm. Before turning on the power supply, we have the gas flowing into the quartz tube for 5 min. Industrial grade (99.99%) of the Air/He/O_2/N_2/Ar gas is used.

III. Experimental Results

A. Ignition of the Plasma

Fig. 2(a) and (b) shows the typical I–V waveforms obtained under the exact similar experimental conditions. It shows clearly that several voltage and current spikes appear for a single voltage pulse. The interval between adjacent current pulses is $\sim$50 ns, and the pulsewidth of each following current spike is $\sim$5 ns. Because of the stochastic nature of air breakdown, the ignition time changes randomly, as shown in Fig. 2(a) and (b). Under these experimental conditions, the appearing time of the first current pulse changes from $\sim$150 to 700 ns, whereas the breakdown voltage V_3 increases from $\sim$2 to 4 kV. The first discharge delay times in Fig. 2(a) and (b) are 200 and 420 ns, respectively. Studies on the discharge breakdown delay time shows that this delay time is relative to the seed electron in the discharging gap, the gap length, gas pressure, working gas, and so on [21]–[23]. In this case, it may due to the seed electrons remaining in the discharge gap. For the first breakdown, the breakdown voltage V_3 and the peak current have the largest amplitude. On the other hand, although the first breakdown voltage V_3 for different delay time is different, the following pulses have almost the same amplitude. The breakdown voltage V_3 of the following discharge pulses is nearly the same, which is $\sim$900 V.

For every applied voltage pulse, the later the first breakdown appears, the larger the amplitudes of the breakdown voltage V_3 and the current because the longer the charging time of the capacitor of the gas gap, the higher the voltage V_3 across the gas gap. Fig. 2(c) shows the plots of the amplitudes of the first breakdown voltage V_3 and current versus delay time of the first breakdown. This figure shows the stochastic but statistic properties of air breakdown under submicroseconds pulsed directed current voltages. It is noteworthy to point out that, after the first discharge pulse, there are many following pulses, but the following pulses only last for some time rather than during the rest of voltage V_1 on time. When no more microdischarge appears, V_3 keeps no obvious change. It is $\sim$900 V until the falling edge of the apply voltage V_1.

B. Effects of Applied Voltage and the Pulsewidth on the Plasma Characteristics

In the next, the discharging gap is still fixed at 0.5 mm, and the working gas is ambient air. Initially, the pulse frequency and pulsewidth are fixed at 8 kHz and 2000 ns, respectively. The applied voltage V_1 varies from 4 to 9 kV. With the increase

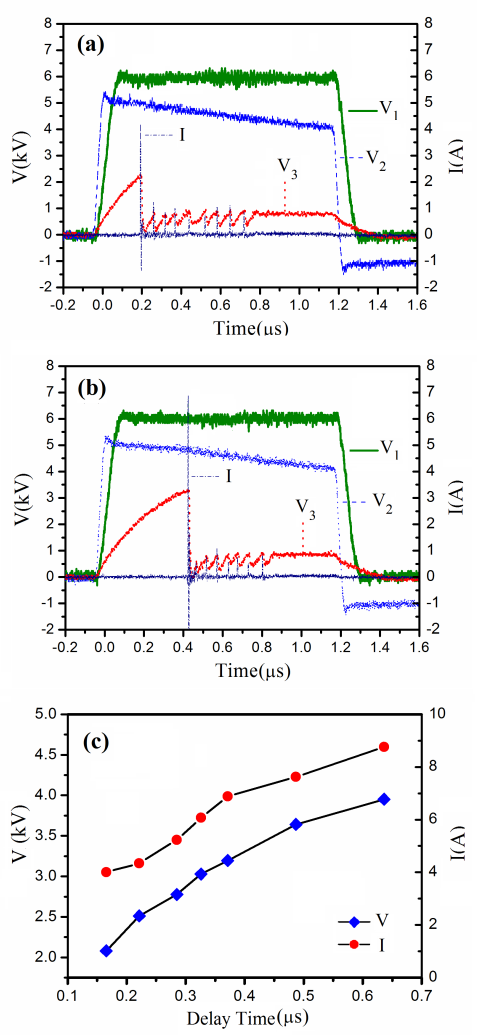

Fig. 2. (a) and (b) Two typical discharge I–V waveforms for the same experimental conditions. The breakdown delay time for (a) and (b) are 0.2 and 0.42 μs, respectively. (c) I–V amplitudes of the first pulse versus the delay time. Gap distance d is fixed at 0.5 mm.

of the applied voltage V_1, the first discharge appears earlier, the first breakdown voltage V_3 and the peak current decrease. However, the amplitude of the breakdown voltage of the following spikes V_3 does not significantly change with the applied voltage V_1. On the other hand, the intervals between the following current pulses decrease with the increasing applied voltage V_1. Fig. 3 shows the time intervals between the following current pulses generated at different applied voltage V_1. It is $\sim$85 ns between the following current pulses when applied voltage V_1 is 4 kV, it decreases to 48 ns for V_1 of 9 kV. In other words, the frequency of the following current pulses increase with the increase of the apply voltage V_1, which is consistent with the characteristics of the Trichel pulses. The intervals between the following pulses in our experiments are, however, in the order of tens of nanoseconds, whereas for the Trichel pulse it is in the order of several microseconds.

With the increase of the pulsewidth, the discharge becomes more and more stable, and the first discharge tends to appear early. The intervals between the following discharge pulses

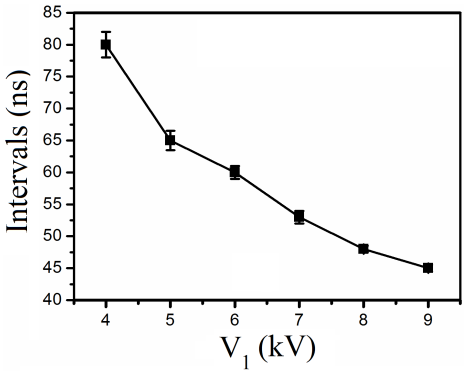

Fig. 3. Intervals between adjacent current pulses versus apply voltage V_1 for applied pulse frequency of 8 kHZ and gas gap of 0.5 mm.

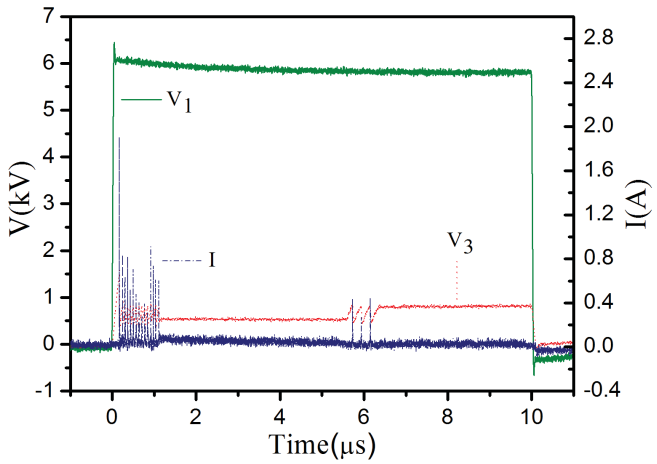

Fig. 4. Multiple discharging pulses sequence for much longer applied pulsewidth for gap distance d of 0.5 mm and applied pulse frequency of 8 kHz.

become longer. With the increasing pulsewidth of the applied voltage V_1, another discharge pulse sequence appears, as shown in Fig. 4. The time interval between the two discharge sequences is $\sim 6\ \mu$s, corresponding to a frequency of 167 kHz. Dubois *et al.* [24] obtained a pulse frequency of ~ 12 kHz in an atmospheric positive corona discharge in air for discharge gap of 9 mm.

C. Effects of the Discharging Gap on the Discharge Characteristics

To understand how the discharge gap affect the plasma characteristics, the plasma for different gaps of 0.1, 0.3, 0.5, and 1 mm is studied for applied voltage of 6 kV, pulsewidth of 1000 ns, and pulse frequency of 8 kHz. Experimental results show that the discharging gap affects the interval of nearby pulses and the pulsewidth of the current. Fig. 5 shows the interval between nearby pulses and the pulsewidth of the current for different discharge gaps. As shown in Fig. 5, the intervals between nearby pulses increase from 37 to 55 ns, and the half-width-half-maximum (HWHM) of the current increases from ~ 1.5 to 8.2 ns when the discharge gap increases from 0.1 to 1 mm.

As we know, in a dc corona discharge, to ignite the next discharge, all the positive ions in the discharge channel have to

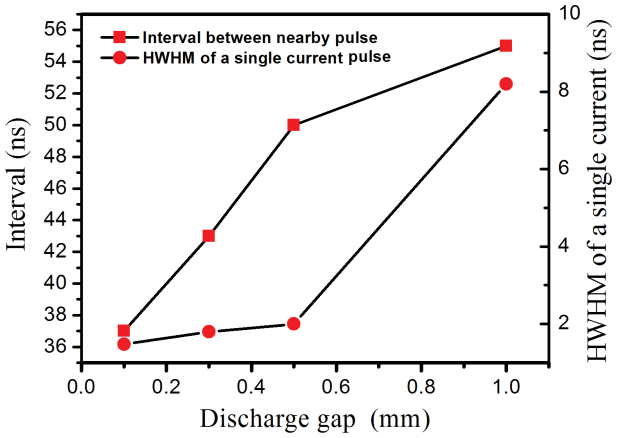

Fig. 5. Intervals between adjacent current pulses and HWHM of a single pulse versus gas gaps for applied voltage of 6 kV, pulsewidth of 1000 ns and pulse frequency of 8 kHz.

be removed by drifting to the cathode. The ion drift mobility μ_i can be expressed as follows:

$$\mu_i = \frac{36\sqrt{1+M/M_i}}{p[\text{atm}]\sqrt{(\alpha/\alpha_0^3)A}}\frac{\text{cm}^2}{V\cdot s} \tag{1}$$

where M is mass of gas molecule and M_i mass of the ion, α/α_0^3 about 10 for N_2 and O_2 plasma [25], A is the molecular weight of the gas. For the ion drift velocity $\upsilon = \mu_i E$, we assume the electric field along the gap is uniform. Then, we obtain $E = 1.2 \times 10^4$ V/cm for 0.5-mm long gas gap. Thus, the removing time of the positive ions (usually N_2^+, hence $M/M_i = 0.5$) in air is ~ 75 ns, which is close to the experimental value of 50 ns. Regarding the pulsewidth of the current, for the 0.5-mm long gas gap, in air, the electron drift velocity is $\sim 7.11 \times 10^5$ m/s, thus it will take ~ 1.5 ns for an electron to pass the gas gap, which is on the same order of our experimental results. Hence, it is reasonable to assume that for each current pulse there is only one electron avalanche, the electrons generated by the electron avalanche pass the gas gap to form the discharge current pulse. Then, the discharge quenches until the positive ions are removed from the gap by drifting under electric field. It is found that (not shown here) numbers of the current pulses in a discharge sequence reduces as the discharge gap increases. When the discharge gap is increased to > 1 mm it becomes a single current pulse other than multiple discharges, which is like the traditional positive corona discharge.

D. Discharges in Different Gases

Researchers have found that regular Trichel pulses only exist in electronegative gasses or their mixtures [26]. To know whether the discharge current pulses reported in this paper has the similar characteristics or not, the plasma characteristics for different gas mixtures are investigated. Fig. 6(a)–(f) shows the I–V waveforms for working gas of He, He/O_2 (3%), He/O_2 (8%), Ar, N_2, and O_2, respectively. During the experiments, the needle is put inside a hermetic cylindrical jar, and the flow rate is kept at 200 sccm. It shows that, when He is used, there

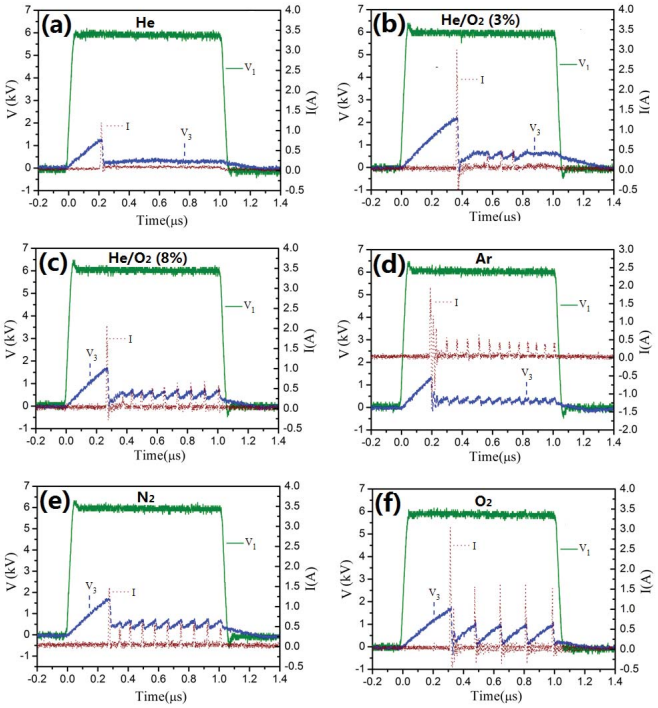

Fig. 6. Current and voltage waveforms for different working gasses. (a)–(f) He, He/O_2 (3%), He/O_2 (8%), Ar, N_2, and O_2, respectively. Gap distance of 0.5 mm and pulse frequency of 8 kHz.

is only one discharge current pulse for all different discharge conditions. The discharge current pulse is different from that shown above in the case of air as working gas. The current has a lower peak value and wider pulsewidth. In addition, it is worthy to point out that the delay time of the current pulse and the current waveform are stable. In other word, the experiment is repeatable.

When a small percentage of O_2 is added to the He gas, multiple discharges appear, as shown in Fig. 6(b) and (c). According to this observation, the multiple discharges are due to the electronegative gas O_2, which is similar with the traditional Trichel pulse. To view if this is true or not, working gas of Ar, N_2, and O_2 are tested. As shown in Fig. 6(d)–(f), there are also multiple discharges for the three different types of working gas. The time interval between nearby current pulse in O_2 is the longest, followed by N_2, and finally by Ar.

When O_2 is used, the electrons could attach to O or O_2, through the reactions $O_2 + e \rightarrow O^- + O$, and $O_2 + e + M \rightarrow O_2^- + M$, which lower down the electron drift velocity and takes more time to breakdown the gas gap, and results in the wider current pulsewidth. In the meantime, electrons attached to O^- or O_2^-, have much lower drift velocity. Although passing the gas gap, they could also recombine with positive ions. This could explain why O_2 has the longest time intervals between nearby current pulse.

IV. Discussion

Corona discharges could be ignited on sharp edge electrode, sharp points (like a tip of a needle) or on thin wires as long as electric field is strong enough to break down the gas [27]. Both negative and positive pin-to-plane dc corona discharges were researched for many years by different groups including Trichel, Loeb Fieux, Lama, *et al.* [28]–[32]. The negative point corona discharges were studied by Trichel (1938) [28], which are characterized by regularly recurring pulses. The discharge propagates radically and is then chocked off by the accumulated space charges [33]. Corona discharge in air at atmospheric pressure has a fast rising time of order 1 ns and a relatively long time interval between pulses [34]. The time interval between pulses is usually in the order of several microseconds, much longer than that the value (~ 50 ns) obtained in discharge reported in this paper.

For negative corona discharge, researchers investigated the effect of various parameters on the characteristics of Trichel pulse [35], [36]. Loeb *et al.* [26] concluded that the Trichel pulses only appear in electronegative gas discharge. Under certain conditions the current of negative point-to-plane corona discharge in electronegative gases consist of a series of regular current pulses of short duration ($\sim$20–100 ns) with repetition frequencies $\sim$ 20–100 kHz [37]. Our experimental results show that regular pulses are also observed in gases such as Ar and N_2, and have shorter duration with higher repetition frequencies. It indicates that the discharge observed in our experiments have different mechanism from that of the traditional Trichel pulses.

Positive pin-to-plane corona and pulsed corona discharges, which are similar with the discharges investigated in this paper, are also researched by different groups [38]–[41]. With the increase of the applied voltages, positive corona is characterized as follows: 1) an intermittent (geiger counter) regime. In this regime, the current depends on the number of external triggering electrons introduced into the gap and on space charge limitation of the individual discharges; 2) a steady burst corona regime, while the current is independent on external ionization; and 3) breakdown streamers [42]. The positive corona discharge currents are a series of irregular pulses with small peak value ($\sim$ 10 mA) and repetitive frequency in the range of 10–30 kHz [43]–[47], which is consistent with the results of the long time duration voltage pulse between two discharge sequences. As analysis shown above, the discharge in our experiments is similar to the normal positive corona. It has, however, its own characteristics. The current pulses within a discharge sequence are more regular and the repetition frequency is much higher (tens of MHz or even higher).

V. Conclusion

The electrical characteristics of an atmospheric pressure pulsed plasma needle were investigated in this paper. A sequence current pulse was observed for one applied voltage pulse. It was found that the first current pulse appeared randomly, and the amplitude of the voltage on the needle V_3 before first breakdown and the discharge current increased with the increase of the breakdown delay time. After the first breakdown, the time intervals between the following nearby current pulses increased with the apply voltage and the gas gap. In addition, the time intervals between the following

nearby current pulses also depended on the working gasses. The pulsewidth of the current increased with the discharge gap. It was also found that there was always only a single discharge pulse for one applied voltage pulse in He, but a sequence of current pulses for all the other working gasses (He /O_2 mixtures, Ar, N_2, O_2, and air).

REFERENCES

[1] M. Laroussi, "Low temperature plasma-based sterilization: Overview and state-of-the-art," *Plasma Process Polymers*, vol. 2, no. 5, pp. 391–400, 2005.

[2] M. Kong, G. Kroesen, G. Morfill, T. Nosenko, T. Shimizu, J. Dijk, and J. Zimmermann, "Plasma medicine: An introductory review," *New J. Phys.*, vol. 11, no. 11, p. 115012, Nov. 2009.

[3] W. Chen, J. Huang, N. Du, X. Liu, X. Wang, G. Lv, G. Zhang, L. Guo, and S. Yang, "Treatment of Enterococcus faecalis bacteria by a helium atmospheric cold plasma brush with oxygen addition," *J. Appl. Phys.*, vol. 112, no. 1, pp. 013304-1–013304-4, Jul. 2012.

[4] I. Levchenko, K. Ostrikov, and E. Tam, "Uniformity of postprocessing of dense nanotube arrays by neutral and ion fluxes," *Appl. Phys. Lett.*, vol. 89, no. 22, pp. 223108-1–223108-3, Nov. 2006.

[5] G. Fridman, G. Friedman, A. Gutsol, A. B. Shekhter, V. N. Vasilets, and A. Fridman, "Applied plasma medicine," *Plasma Processes Polymers*, vol. 5, no. 6, pp. 503–533, Aug. 2008.

[6] K. Ostrikov, "Colloquium: Reactive plasmas as a versatile nanofabrication too," *Rev. Modern Phys.*, vol. 77, no. 2, pp. 489–511, 2005.

[7] C. Jiang, A. Mohamed, R. Stark, J. Yuan, and K. Schoenbach, "Removal of volatile organic compounds in atmospheric pressure air by means of direct current glow discharges," *IEEE Trans. Plasma Sci.*, vol. 33, no. 4, pp. 1416–1425, Aug. 2005.

[8] K. Ostrikov, "Colloquium: Reactive plasmas as a versatile nanofabrication tool," *Rev. Modern Phys.*, vol. 77, no. 2, pp. 489–511, Jun. 2005.

[9] D. Mariotti, "Nonequilibrium and effect of gas mixtures in an atmospheric microplasma," *Appl. Phys. Lett.*, vol. 92, no. 15, pp. 151505-1–151505-3, Apr. 2008.

[10] M. Teschke, J. Kedzierski, E. G. Finantu-Dinu, D. Korzec, and J. Engemann, "High-speed photographs of a dielectric barrier atmospheric pressure plasma jet," *IEEE Trans. Plasma Sci.*, vol. 33, no. 2, pp. 310–311, Apr. 2005.

[11] B. Sands, B. Ganguly, and K. Tachibana, "A streamer-like atmospheric pressure plasma jet," *Appl. Phys. Lett.*, vol. 92, no. 15, pp. 151503-1–151503-3, Apr. 2008.

[12] G. Naidis, "Modelling of streamer propagation in atmospheric-pressure helium plasma jets," *J. Phys. D, Appl. Phys.*, vol. 43, no. 40, p. 402001, Oct. 2010.

[13] P. Bruggeman and C. Leys, "Non-thermal plasmas in and in contact with liquids," *J. Phys. D, Appl. Phys.*, vol. 42, no. 5, p. 053001, Mar. 2009.

[14] W. Zhu, Q. Li, X. Zhu, and Y. Pu, "Characteristics of atmospheric pressure plasma jets emerging into ambient air and helium," *J. Phys. D, Appl. Phys.*, vol. 42, no. 20, p. 202002, Oct. 2009.

[15] L. Ji, D. Liu, Y. Song, and J. Niu, "Atmospheric pressure dielectric barrier microplasmas inside hollow-core optical fibers," *J. Appl. Phys.*, vol. 111, no. 7, pp. 073304-1–073304-6, Apr. 2012.

[16] X. Zhou, Z. Xiong, and Y. Cao, "The antimicrobial activity of an atmospheric-pressure room-temperature plasma in a simulated root-canal model infected with Enterococcus faecalis," *IEEE Trans. Plasma Sci.*, vol. 38, no. 12, pp. 3370–3374, Dec. 2010.

[17] M. Keidar, R. Walk, A. Shashurin, P. Srinivasan, A. Sandler, S. Dasgupta, R. Ravi, R. Guerrero-Preston, and B. Trink, "Cold plasma selectivity and the possibility of a paradigm shift in cancer therapy," *Brit. J. Cancer*, vol. 105, pp. 1295–1301, Oct. 2011.

[18] S. Wu, X. Lu, Z. Xiong, and Y. Pan, "A touchable pulsed air plasma plume driven by DC power supply," *IEEE Trans. Plasma Sci.*, vol. 38, no. 12, pp. 3404–3408, Dec. 2010.

[19] J. F. Kolb, A.-A. H. Mohamed, and R. O. Price, "Cold atmospheric pressure air plasma jet for medical applications," *Appl. Phys. Lett.*, vol. 92, no. 24, pp. 241501-1–241501-3, Jun. 2008.

[20] X. Lu, Z. Xiong, and F. Zhao, "A simple atmospheric pressure room-temperature air plasma needle device for biomedical applications," *Appl. Phys. Lett.*, vol. 95, no. 18, pp. 181501-1–181501-3, Nov. 2009.

[21] L. G. Bychkova, Y. I. Bychkov, and G. A. Mesyats, "Rapid increase in the delay time for the breakdown of gas-filled gaps in high electric fields," *Soviet Phys. J.*, vol. 12, no. 2, pp. 162–164, Feb. 1969.

[22] L. G. Bychkova, Y. I. Bychkov, G. A. Mesyats, and Y. Y. Yurike, "Electron-optics study of the development of an electric discharge in a gas at high-electric field intensities and with one-electron ignition," *Soviet Phys. J.*, vol. 12, no. 11, pp. 1389–1391, Nov. 1969.

[23] Y. P. Raizer, *Gas Discharge Physics*. New York, NY, USA: Springe-Verlag, 1991.

[24] D. Dubois, N. Merbahi, O. Eichwald, M. Yousfi, and M. Benhenni, "Electrical analysis of positive corona discharge in air and N_2, O_2, and CO_2 mixture," *J. Appl. Phys.*, vol. 101, no. 5, pp. 053304-1–053304-9, Mar. 2007.

[25] Y. P. Raizer, *Gas Discharge Physics*. Berlin, Germany: Springer-Verlag, 1991.

[26] L. B. Loeb, A. F. Kip, and G. G. Hudson, "Pulses in negative point-to-plane corona," *Phys. Rev.*, vol. 60, no. 10, pp. 714–722, Nov. 1941.

[27] A. Fridman and L. A. Kennedy, *Plasma Physics and Engineering*. New York: Taylor & Francis, 2004.

[28] G. W. Trichel, "The mechanism of the negative point to plane corona near onset," *Phys. Rev.*, vol. 54, no. 12, pp. 1078–1084, Dec. 1938.

[29] L. B. Loeb, A. F. Kip, G. G. Hudson, and W. H. Bennet, "Pulses in negative point-to-plane corona," *Phys. Rev.*, vol. 60, no. 10, pp. 714–722, Nov. 1941.

[30] L. B. Loeb, *Electrical Coronas*. Berkeley, CA, USA: Univ. of California Press, 1965.

[31] R. Fieux, and M. Boutteau, "Reseaux electriques materiels electriques," *Bull. Directory Etude Rech. Serie B*, vol. 15, no. 2, pp. 55–88, 1970.

[32] W. L. Lama and C. F. Gallo, "'Trichel' current pulses from negative needle-to-plane coronas," *J. Appl. Phys.*, vol. 45, pp. 103–113, Jan. 1974.

[33] T. M. Giao and J. B. Jordon, "Modes of corona discharges in air," *IEEE Trans. Power App. Syst.*, vol. 87, no. 5, pp. 1207–1215, May 1968.

[34] L. Aubrecht, J. Kollerand, and A. Zahoranova, "Trichel pulses in negative corona discharge on trees," *J. Phys. D, Appl. Phys.*, vol. 32, no. 18, p. L87, Sep. 1999.

[35] R. Fieux and M. Boutteau, "Phenomenes de predecharges entre une pointe et un plan dans i'air sous tension continue bulletin de la direction des etudes el recherches," *EDF Series B*, vol. 15, no. 2, pp. 55–88, 1970.

[36] W. L. Lama and C. F. Gallo, "Systematic study of the electrical characteristics of the 'Trichel' current pulses from negative needle-to-plane coronas," *J. Appl. Phys.*, vol. 45, no. 1, pp. 103–124, Jul. 1974.

[37] D. A. Scott and G. N. Haddad, "Negative corona in nitrogen-oxygen mixtures," *J. Phys. D, Appl. Phys.*, vol. 20, no. 8, pp. 1039–1044, Aug. 1987.

[38] J. Khun and S. Pekarek, "Dynamic characteristics of positive hollow needle to plate atmospheric pressure discharge," *Czechoslovak J. Phys.*, vol. 56, no. 2, pp. B830–B836, Oct. 2006.

[39] R. Ono and Y. T. TetsujiOda, "Effect of humidity on gas temperature in the afterglow of pulsed positive corona discharge," *Plasma Sour. Sci. Technol.*, vol. 19, no. 1, pp. 015009-1–015009-5, Feb. 2010.

[40] M. R. Amin, "Fast time analysis of intermittent point-to-plane corona in air I: The positive point burst pulse corona," *J. Appl. Phys.*, vol. 25, no. 2, pp. 210–217, 1954.

[41] M. R. Amin, "Fast time analysis of intermittent point-to-plane corona in air. II: The positive pre-onset streamer corona," *J. Appl. Phys.*, vol. 25, no. 3, pp. 358–364, 1954.

[42] W. N. English, "Positive and negative point-to-plane corona in air," *Phys. Rev.*, vol. 74, no. 2, pp. 170–178, Jul. 1948.

[43] Z. Machala, I. Jedlovsky, and V. Martisovits, "DC discharges in atmospheric air and their transitions," *IEEE Trans. Plasma Sci.*, vol. 36, no. 4, pp. 918–919, Aug. 2008.

[44] Z. Machala, I. Jedlovsky, L. Chladekova, B. Pongrac, D. Giertl, M. Janda, L. Sikurova, and P. Polcic, "DC discharges in atmospheric air for bio-decontamination—Spectroscopic methods for mechanism identification," *Eur. Phys. J. D*, vol. 54, no. 2, pp. 195–204, Aug. 2009.

[45] E. M. van Veldhuizen and W. R. Rutgers, "Pulsed positive corona streamer propagation and branching," *J. Phys. D, Appl. Phys.*, vol. 35, no. 17, p. 2169, Sep. 2002.

[46] P. Tardiveau, E. Marode, and A. Agneray, "Tracking an individual streamer branch among others in a pulsed induced discharge," *J. Phys. D, Appl. Phys.*, vol. 35, no. 21, p. 2823, 2002.

[47] W. J. Yi and P. F. Williams, "Experimental study of streamers in pure N_2 and N_2/O_2 mixtures and a ≈13 cm gap," *J. Phys. D, Appl. Phys.*, vol. 35, no. 3, p. 205, Feb. 2002.

Authors' biographies and photographs not available at the time of publication.